Current Applied Physics 12 (2012) 65–68

Contents lists available at ScienceDirect

Current Applied Physics

journal homepage: www.elsevier.com/locate/cap

Magnetic properties of one-dimensional embedded nickel nanostructures in gold nanowires

S. Ishrat [a], K. Maaz [a], Rong Chen [a], Soo Hyun Kim [b], M.H. Jung [b], Gil-Ho Kim [a,*]

[a] School of Information and Communication Engineering, Sungkyunkwan Advanced Institute of Nanotechnology (SAINT), Sungkyunkwan University, Suwon 440-746, Republic of Korea
[b] Department of Physics, Sogang University, Seoul 121-742, Republic of Korea

ARTICLE INFO

Article history:
Received 31 March 2011
Accepted 25 April 2011
Available online 5 May 2011

Keywords:
Ni nanowires
Electrodeposition
Magnetic properties
Template synthesis

ABSTRACT

Magnetic nanostructures of nickel embedded in gold were successfully fabricated by electrochemical deposition in porous alumina templates. Structural characterization of the samples confirmed the formation of pure phase, crystalline multi-segmented Au–Ni–Au nanowires. Magnetic characterization of the wires reveals that ferromagnetism arises as a result of Ni embedded in Au segments. An interesting behavior of coercivity was observed that showed a rapid decrease of coercivity for smaller Ni segments while a monotonic decrease was found for the larger segments. Finally, the saturation magnetization of the wires exhibited a slower increase for smaller Ni segments while a sharp increase was observed for larger Ni segments.

1. Introduction

Recently multi-segment nanowires (NWs) are the subject of immense interest because of their novel physical and chemical properties that are different from their bulk counter parts. Various properties of materials at the nano-scale can be tailored by suitable choice and length of one (e.g. ferromagnetic) material embedded in other (e.g. nonmagnetic) material. Such materials have the interesting spin dependent electrical properties that can be used as the *spintronics* device. While in computer industry these NWs can be used for magnetic storage devices and transistor applications where the length and diameter of the wires is controlled carefully by controlling the deposition of charges during the fabrication process. In the recent years, Ni has attracted much attention due to its potential applications as ultra high density magnetic recording media. While growing these NWs in porous alumina (AAO) templates, among others e.g. polycarbonate etc. AAO is more convenient to use as the hosting material for growing of NWs because it has high pore density and relatively smaller size distribution compared to other templates. Magnetic NWs of Ni grown in porous alumina have uniaxial anisotropy with direction of easy axis of magnetization lying along the wire-long axis that arises as a result of the shape anisotropy in cylindrical NWs [1]. The advantage of this method over the others is because of its relatively less time consumption and cheaper as compare to other fabrication methods. Moreover, this process can easily be carried out at the atmospheric conditions with varying segment length that can be fabricated by varying the reduction potentials during the growth of the wires. It is noticeable, in this process the interface between different segments can be controlled by changing the shape of the electrical pulse responsible for ions reduction in the solution.

In embedded NWs the analysis in multilayer system leads to several interesting phenomenon that are very important from their application point of view. In these wires, a well defined hard and easy axis of magnetization exists due to their strong shape anisotropy, especially in cylindrical NWs that plays a crucial role in determining various magnetic properties in such systems. Competition between the shape and magnetocrystalline anisotropies can be tailored to study magnetic properties in these wires. The most significant properties of embedded NWs, namely magnetic saturation, coercivity (H*c*), magnetization and loss etc. change drastically as the diameter or length of ferromagnetic(FM) segment is reduced to the nanometric range [2–4]. From the application point of view, the magnetic character of NWs depends crucially on diameter, shape, purity and magnetic stability of these wires. These should be single domain, of pure phase, suitable coercivity, moderate magnetization and stable blocking temperatures. In recording applications, the superparamagnetic blocking temperature of the wires should be well above the room temperature in order to have a stable data recorded in these materials used in magnetic storage applications while in biomedical applications relatively lower blocking temperature is required [5]. There is

* Corresponding author.
E-mail address: ghkim@skku.edu (Gil-Ho Kim).

1567-1739/$ – see front matter © 2011 Elsevier B.V. All rights reserved.
doi:10.1016/j.cap.2011.04.043

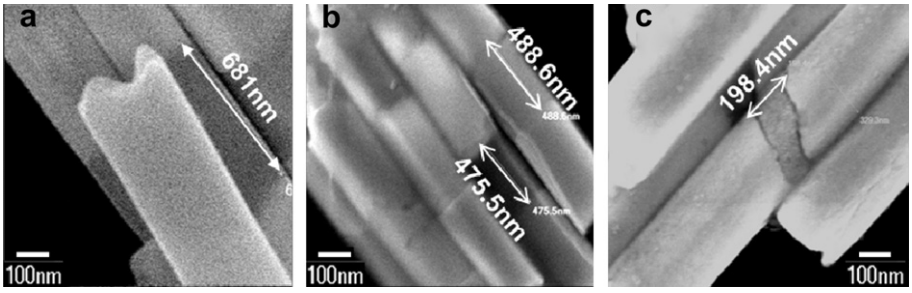

Fig. 1. Field emission SEM image of NW's with (a) 681 nm nickel segment, (b) 475.5 nm Ni segment, and (c) 198.4 nm long Ni segment respectively.

a considerable interest in the magnetism and its related phenomena at the nano-scaled embedded NWs that arise due to many competing interactions that are difficult to differentiate in these wires. These include surface effects, finite size effects, and the inter-wire interactions. It is now well-established that in small diameter wires, on nano-scale, the surface spins play a dominant role regarding their magnetic properties. These spins cause for example, reduction of saturation magnetization (Ms) with decreasing sizes and the enhancement of Hc in these nano-scale materials. It has been shown earlier [6,7] that in nanomaterials, due to the broken symmetries and exchange bonds at the surface, these spins do not follow the core anisotropy direction and become disordered or canted leading to even high anisotropy compared to the core of the materials. Such nanomaterials are generally termed as the core-shell materials, where the core-spins behave like FM and the shell is composed of disordered or canted spins that behaves magnetically different form their core counter parts.

In the present work, Au–Ni–Au NWs were synthesized by electrochemical deposition technique that will be used later for their practical applications as spintronics and chemical sensors. The as-fabricated NWs were characterized by the field emission scanning electron microscope (FESEM), high resolution transmission electron microscopy (HRTEM), X-ray diffraction (XRD), energy-dispersive X-ray spectroscopy (EDS). Magnetic properties were measured using a superconducting quantum interference device magnetometer. Effects of Ni segment length on various magnetic properties like H*c* and M*s* have been studied in detail and the results have been explained in light of the recent results and models for similar NWs.

2. Experimental procedure

Alumina templates with pore diameter of ~400 nm and thickness of ~13 mm were used for deposition of the wires. Prior to the deposition a thin layer of silver was thermally evaporated on one side of the template to make it conductive for the working electrode. Platinum wire and Ag/AgCl served as the counter and reference electrodes respectively. DC cell was used with three-electrode configuration. A constant potential of −0.95 V was applied between the working and reference electrode. For the uniformity of cathode surface, a thin sacrificial Ag layer (~2 μm) was grown on one side of alumina template by electrochemical deposition [8]. The length of gold and nickel segments was adjusted by controlling the quantity of deposited charge through the deposition process [9]. To liberate the NWs from the templates Ag layer was etched in concentrated nitric acid for ~5 min before liberating the wires from the templates. For structure analysis the wires were liberated by dissolving the templates in 3 molar sodium hydroxide solution for about 40 min. The wires were separated by centrifuging and then cleaning with de-ionized water. To get the pure NWs and avoid any impurity the cleaning process was repeated for 4–5 times and then the wires were dried out on the Si/SiO_2 substrate. For FESEM, TEM and XRD analyses the wires were liberated from the templates by dissolving AAO template in NaOH solution while for magnetic measurements the wires were left embedded in the templates.

3. Results and discussion

Fig. 1 shows the FESEM images of the as-prepared embedded NWs. High magnification FESEM image of Au–Ni–Au NWs with average diameter of ~400 nm and various Ni segment lengths as shown in Fig. 1. Fig. 1(a) shows the high resolution FESEM image with Ni segment of ~681 nm while Fig. 1(b) shows the three segments with Ni embedded between the two Au segments. In this case the length of Ni is ~475 nm with wire diameter of ~400 nm. In Fig. 1(c) a smaller segment of Ni is embedded between the gold indicating about 198 nm length of Ni. In FESEM images it is seen that the prepared NWs are cylindrical in shape with uniform cross-section over their whole lengths and wires exhibit homogenous contours. Due to the good quality of the AAO used in this work, the diameter distribution within a given sample was very narrow.

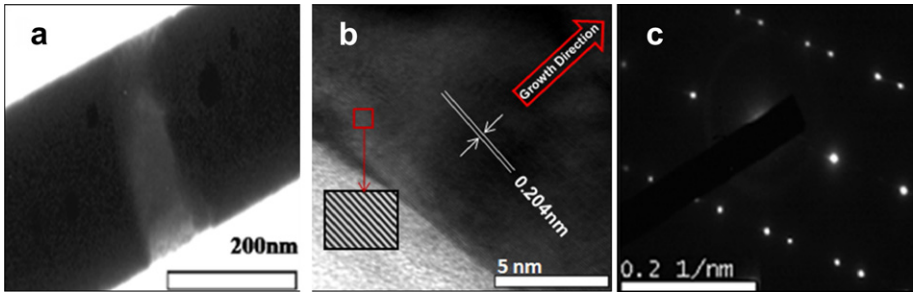

Fig. 2. TEM image of NW's with (a) Ni segment embedded between gold segments. (b) The HRTEM image shows the estimated lattice spacing of ~0.204 nm, while arrow in the figure indicates the growth direction of the wires, and (c) selected area electron diffraction of a segment of a wire.

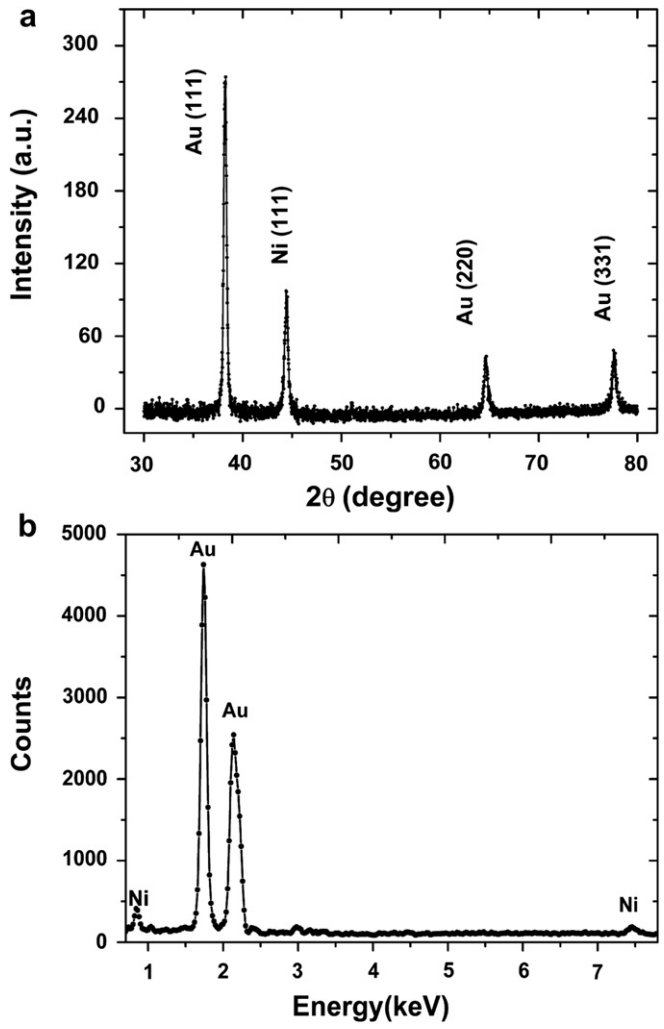

Fig. 3. (a) X-ray diffraction pattern of the wires. (b) EDS results indicating the quantitative presence of various metals in the wires.

Scatter in diameters of the wires was less than 5% of their mean values. The characteristics of the membranes employed are extremely important for fabrication of the wires. The shape of the pores in commercially available membranes is reported to be toothpick- or cigar-like [10,11]. The origin of such shapes is ascribed to the presence of surfactants in the etching solution [12]. The wires prepared in the commercial membranes are reported to be up to a factor 2.5 wider in the central part than at the ends in case of polycarbonate membranes [10] however, in case of AAO templates this distribution is relatively lower as the alumina templates are brittle as compared to PC templates.

Fig. 2 represents the TEM images of embedded Ni NWs that were liberated from the templates by dissolving it in 3 molar sodium hydroxide solution. TEM image shown in Fig. 2(a) represents ~80 nm Ni segment embedded between gold segments with wire diameter of ~400 nm. The lattice parameter estimated from HRTEM was found to be ~0.204 nm that corresponds to *fcc* structured Ni. This was further investigated by XRD analysis and confirmed for metallic *fcc* Ni. Fig. 2(c) shows the selected area electron diffraction (SAED) image of a segment in the wire that indicates the completely single crystalline nature of the fabricated NWs. The arrow shown in Fig. 2(b) pointing the growth direction of the wires. Fig. 3(a) shows the XRD pattern of the wires with $K\alpha$ as the x-ray source. XRD analysis of the wires after liberating from AAO templates shows the (111) reflections at 44.5° that corresponds to *fcc* Ni while other peaks at 38.2°, 64.6°, and 77.6° representing the *fcc* Au. No other peaks were found in the XRD confirming that the embedded NWs are composed of purely crystalline Ni and Au metals. The quantitative presence of various metals in the prepared NWs performed by EDX shown in Fig. 3(b) reveals that the prepared NWs are composed of mainly Ni and Au with a prominent peak of silicon that appears from the substrate material used for the dispersion of the wires. Thus both results of XRD and EDX confirm that our samples are composed of Ni and Au without any impurities.

For magnetic characterization the magnetic hysteresis M (H) loops were taken at 300 K under an applied field of 10 kOe. Fig. 4 shows the M (H) loops for different segment lengths (l = 26, 163, 218, 640 nm) of FM Ni embedded between Au. It is clear in the data

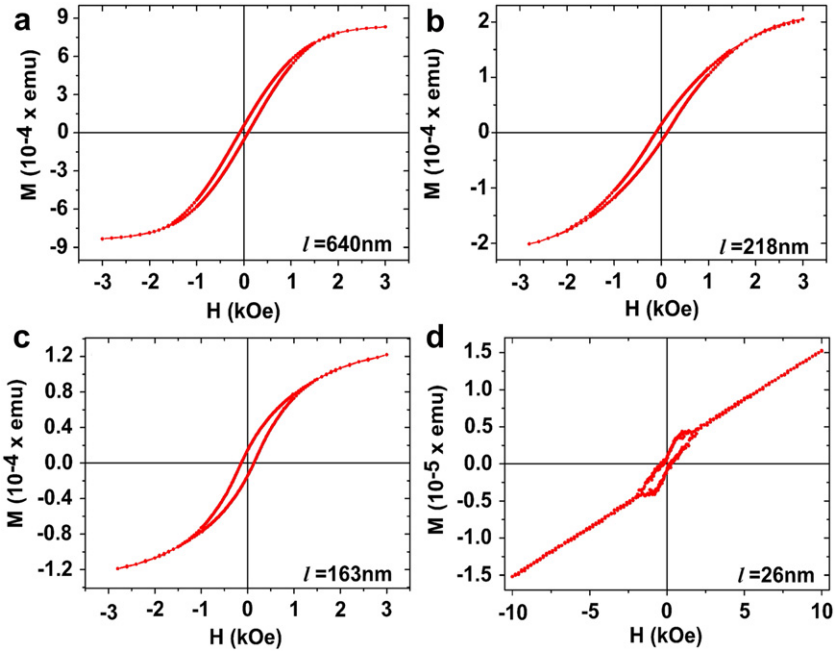

Fig. 4. M (H) loops of ferromagnetic nickel present in gold. The loops were taken at 300 K for different segment lengths. In the figure (a) indicates the NWs with Ni segment 640 nm embedded between gold segments, (b) indicates segment with length of 218 nm. (c) Indicates the segment length 185 nm, while (d) indicates 26 nm long Ni segment.

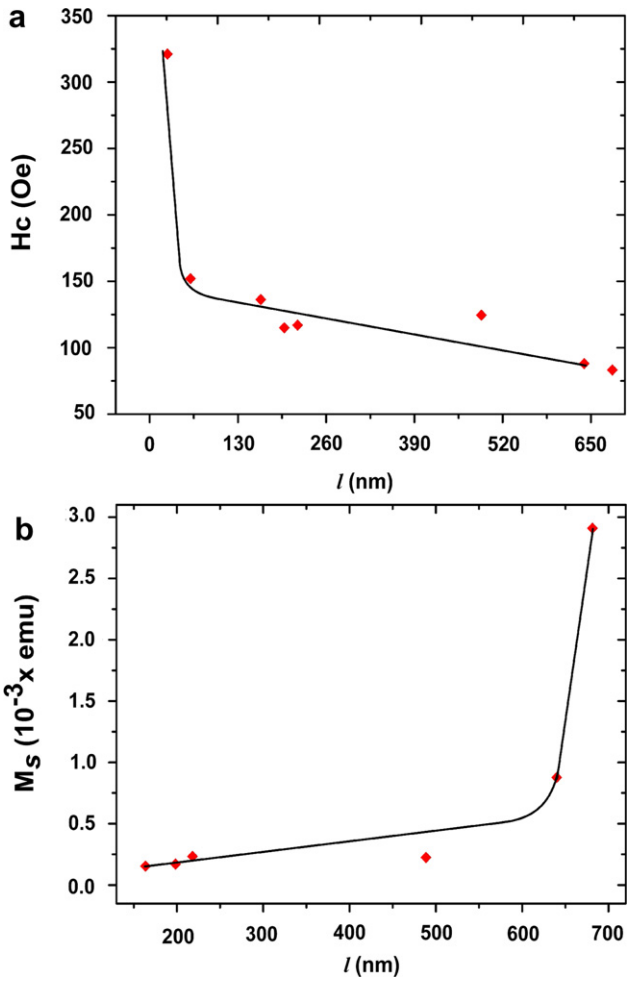

Fig. 5. (a) Coercivity as a function of Ni segment length with same diameter of ~400 nm of the NWs embedded in AAO. (b) Variation of Ms with segmented length for the samples. For smaller Ni segments the values of magnetization was negligibly smaller therefore, not included in the graph.

that the prepared NWs show FM behavior because of Ni portion that is FM in nature. Fig. 5(a) shows the H_C as a function of Ni segment length. In the figure, it is seen that H_C increases monotonically with decreasing Ni segment from 680 nm down to ~160 nm, however, below this value (=~160 nm) of Ni segment length the increase in H_C becomes very fast. From Fig. 5(b), it is seen that M*s* is quite high for large Ni segments (l = ~680 nm), falls rapidly below this value and then attains a slower and monotonic decrease in the range (26–600 nm). The initial increase in H_C for smaller Ni segments in the range 26–160 nm assigned to the departure from the single crystalline NWs to multicrystalline NWs. This occurs in smaller Ni segments when the single crystalline Ni behaves like magnetically single domain and the H_C increases within the premises of Stoner Wohlfarth model for FM materials, while the value of H*c* is expected to be smaller for large Ni segments because the Ni becomes multicrystalline and hence the multidomain in this region. This results in the degradation of H*c* values for large Ni segments. It has been observed that the effective anisotropy constant in case of nanoparticles increases with decreasing sizes according to phenomenological expression ($K_{eff} = K_V + (6/d)K_S$) for the effective anisotropy of spherical nanoparticles. Several other works including simulation and experimental have also supported this expression [13]. If we assume similar behavior in our embedded NWs i.e. an increase in the effective anisotropy constant with reducing Ni segment (from 680 nm down to 26 nm), this would tend to increase the H_C of the wires within the Stoner Wohlfarth picture ($H_C = 2K/M_S$) consistent with the behavior of H_C for smaller segments as shown in Fig. 5(a). For very smaller segments (below ~160 nm) the increase in value of K*s* becomes very high due to the increasing surface effects for smaller segments, that resultantly increases the value of effective anisotropy constant according to the above relation thereby increasing the H_C for smaller Ni segments.

In case of M*s* that decreases by decreasing length of Ni as shown in Fig. 5(b), is clear that for large Ni segments the larger content of FM material embedded in Au causes an increased net magnetization of the wires. As the length of Ni segment decreases, the content of FM Ni decreases that results in smaller M*s* of the wires. In Fig. 5(b) it is seen that the fall in M*s* is high in the beginning while this decrease in M*s* becomes slower for the sizes below ~600 nm. This can be interpreted that for larger segments, above 600 nm, the smaller decrease in length causes a larger decrease in FM Ni that causes a substantial reduction in M*s* of NWs.

4. Conclusion

Controlled one-dimensional Ni nanostructures embedded in Au have been successfully fabricated by electrochemical deposition in AAO templates. Structural characterization of the samples confirmed the formation of pure phase single crystalline Au–Ni–Au NWs. Very high coercivity of the wires has been found for smaller Ni segments that have been attributed to the single domain nature of the wires according to the Stoner Wohlfarth model for ferromagnetic materials. Finally, the high magnetization for larger Ni lengths embedded in gold has been attributed to the larger content of ferromagnetic Ni present in gold that resulted in larger M_S values in the prepared nanowires.

Acknowledgments

This research was supported by World Class University program funded by the Ministry of Education, Science and Technology through the National Research Foundation of Korea (R32-10204).

References

[1] K. Maaz, S. Karim, M. Usman, A. Mumtaz, J. Liu, J.L. Duan, M. Maqbool, Nanoscale Res. Lett. 5 (2010) 1111.
[2] I.M.L. Billas, A. Chatelain, W.A. de Heer, Science 265 (1994) 1682.
[3] D.D. Awschalom, D.P.D. Vincenzo, Phys. Today 43 (1995).
[4] M. George, A.M. John, S.S. Nair, P.A. Joy, M.R. Anantharaman, J. Magn, Magn. Mater. 302 (2006) 190.
[5] K. Maaz, S. Karim, A. Mumtaz, S.K. Hasanain, J. Liu, J.L. Duan, J. Magn, Magn. Mater. 321 (2009) 1838.
[6] R.H. Kodama, A.E. Berkowitz, J. Appl. Phys. 81 (1997) 5552.
[7] R.H. Kodama, A.E. Berkowitz, Phys. Rev. Lett. 77 (1996) 394.
[8] N.V. Hoang, S. Kumar, Gil-Ho Kim, Nanotechnology 20 (2009) 125607.
[9] K. Sungwan, S.L. Kevin, B. Hyun-Mi, K.K. Seong, P. Sungho, Nano Lett. 8 (3) (2008) 800.
[10] C. Schönenberger, B.M.I. van der Zande, L.G.J. Fokkink, M. Henny, C. Schmid, M. Krueger, A. Bachtold, A. Huber, H. Birk, U. Staufer, J. Phys. Chem. B. 101 (1997) 5497.
[11] E. Ferain, R. Legras, Nucl. Instrum. Methods Phys. Res. B. 174 (2001) 116.
[12] P.Y. Apel, I.V. Blonskaya, O.L. Orelovich, S.N. Akimenko, B. Sartowska, S.N. Dmitriev, Colloid J. 66 (6) (2004) 649.
[13] B.R. Pujada, E.H.C.P. Sinnecker, A.M. Rossi, A.P. Guimaraes, J. App. Phys. 93 (2003) 7217.